Journal of Cancer Research and Clinical Oncology
https://doi.org/10.1007/s00432-023-05213-z

RESEARCH

The role of KPNA2 as a monotonically changing differentially expressed gene in the diagnosis, risk stratification, and chemotherapy sensitivity of chronic hepatitis B-liver cirrhosis-hepatocellular carcinoma

Yong Pan[1] · Yiru Zhang[1,3] · Zhengmei Lu[1] · Danwen Jin[2] · Shibo Li[1]

Received: 8 July 2023 / Accepted: 25 July 2023

Abstract

Purpose Chronic hepatitis B-liver cirrhosis-hepatocellular carcinoma (CLH), commonly called the "liver cancer trilogy", is a crucial evolutionary phase in the emergence of hepatocellular carcinoma (HCC) in China. Previous studies on early diagnostic biomarkers of HCC were limited to the end-stage of HCC and did not focus on the evolutionary process of CLH.

Methods 11 monotonically changing differentially expressed genes (MCDEGs) highly correlated with CLH were screened through bioinformatic analysis and KPNA2 was identified for further research. The serum KPNA2 expression in different CLH states was detected by Enzyme linked immunosorbent assay (ELISA). A nomogram model was constructed using univariate and multivariate Cox regression methods.

Results The single-cell RNA-seq and bulk RNA-seq revealed that KPNA2 related to immune infiltration in HCC and may participate in cell cycle pathways in HCC. The serum KPNA2 expression was monotonically upregulated in CLH and was valuable for diagnosing different CLH states. Besides, chronic hepatitis B(CHB) patients, liver cirrhosis (LC) patients, and HCC patients were classified into subgroups with distinct serum KPNA2 expressions. Accordingly, patients with different serum KPNA2 expressions displayed various clinicopathological features. The AUC value of the nomogram model was 0.959 in predicting the likelihood of developing HCC in CHB patients or LC patients. Finally, we found that KPNA2 expression was negatively correlated with the IC_{50} of four chemotherapeutic drugs in HCC.

Conclusion KPNA2 was a novel serum biomarker for diagnosing different CLH states, monitoring the dynamic evolution of CLH, and a new therapeutic target for intervening in the progression of CLH.

Keywords Hepatocellular carcinoma · Karyopherin subunit alpha 2 · Biomarker · Diagnosis · Risk stratification

Introduction

Primary liver cancer is the third most common cause of cancer-related fatalities worldwide, posing a severe threat to human health and life (Sung et al. 2021). Hepatocellular carcinoma (HCC) is the most prevalent subtype of liver cancer, making up 85–90% of all cases (Mehta 2020; Wang et al. 2017). Chronic hepatitis B-liver cirrhosis-hepatocellular carcinoma (CLH), commonly called the "liver cancer trilogy", is a crucial evolutionary phase in the emergence of HCC in China (Xu et al. 2023; Hsu et al. 2023). Chronic hepatitis B (CHB) often causes recurrent liver damage, necrosis, and inflammation, with diffuse fibrosis, nodules, and pseudolobules in the liver tissue, eventually progressing to cirrhosis (Stroffolini and Stroffolini 2023). Liver cirrhosis (LC) is a

✉ Shibo Li
lsb0398@126.com

1 Department of Infectious Disease, Zhoushan Hospital, Wenzhou Medical University, 739 Dingshen Rd, Zhoushan City 316021, China

2 Pathological Diagnosis Center, Zhoushan Hospital, Wenzhou Medical University, 739 Dingshen Rd, Zhoushan City 316021, China

3 State Key Laboratory for the Diagnosis and Treatment of Infectious Diseases, The First Affiliated Hospital, Zhejiang University School of Medicine, 79 Qingchun Rd, Hangzhou City 310003, China

Published online: 01 August 2023

major risk indicator for HCC, mainly because of a strong inflammatory milieu that encourages carcinogenesis in the sclerotic tissue (Pinter et al. 2016).

Due to the lack of distinct symptoms in the early stages and early diagnostic markers, most HCC patients are detected in advanced stages with a poor prognosis. Serological screening and diagnostic markers for HCC that are commonly used now in clinical practice include AFP (Lim et al. 2022), AFP-L3 (Malaguarnera et al. 2010), DCP (Tanaka et al. 2013) etc. However, they do not sufficiently reflect the dynamic development of CLH as a disease process and are not sensitive or specific enough. Hence, biomarkers that could predict CLH progression are urgently required to improve the prognosis of HCC patients.

Genes that show monotonically increasing or decreasing expression with significant differences during the course of CLH are defined as monotonically changing differentially expressed genes (MCDEGs), which may be closely associated with disease progression and may be utilized as biomarkers to predict disease progression and prognosis. Karyopherin subunit alpha 2 (KPNA2) is one of the significant MCDEGs screened. KPNA2, one of the seven adhesion family members, is mostly located in the cytoplasm and nucleus (Zhang et al. 2015). KPNA2 participates in the body's biological functions, such as differentiation (Li et al. 2008) viral infection (Qu et al. 2004), immunomodulation (O'Brien et al. 2011), and metabolic response (Cassany et al. 2004) etc. In recent years, surprisingly numerous bioinformatic analyses and experimental evidence have clarified that KPNA2 exerted cancer-promoting effect on HCC and was implicated in the molecular process that led to the development of HCC (Zan et al. 2019; Guo et al. 2019). Zhang et al. found that KPNA2 was overexpressed in the early stages of HCC and was an independent predictor of poor prognosis in HCC (Zhang et al. 2021). Chen et al. confirmed that KPNA2 could facilitate tumor progression in HCC through the AKT signaling pathway in a hypoxic environment (Chen et al. 2021) which was compatible with the outcomes of previous experiments (Wang et al. 2019). However, the diagnostic and prognostic value of KPNA2 has not been fully demonstrated.

In our study, we screened eleven MCDEGs highly correlated with CLH through bioinformatic analysis and identified KPNA2 for further research. We explored the significance of KPNA2 using survival, pathway enrichment, gene network interaction and immune infiltration analysis. Moreover, we detected KPNA2 expression levels in the serum samples from CHB patients, LC patients, and HCC patients, respectively, and demonstrated its diagnostic value for distinguishing different CLH states. In addition, we delved into the association between serum KPNA2 expression and prognostic variables in CHB, LC, and HCC, respectively, and constructed a predictive nomogram model for CLH. Herein, we, for the first time, developed a holistic approach to research the CLH process from the perspective of MCDEGs. Hopefully, our study will provide a new serum biomarker for monitoring the dynamic evolution of CLH, a new therapeutic target for intervening in the progression of CLH, and a positive impact on the early prevention and treatment of HCC.

Materials and methods

Patient information and sample collection

A total of 205 serum samples with clinical information (86 samples from CHB patients, 56 samples from LC patients, and 63 samples from primary HCC patients) were included in the study. The serum samples were collected between September 2021 and May 2023 from Wenzhou Medical University Affiliated Zhoushan Hospital (Zhoushan, China). The serum was centrifuged and stored at – 80 °C until testing. Meanwhile, the study subjects' demographic and clinical data, radiographic examinations, and laboratory tests were obtained from hospital electronic medical records. It should be noted that all HCC and LC patients were developed from CHB, and serum samples from HCC patients were collected before the surgery. All patients met diagnostic criteria according to the latest Chinese clinical guidelines. Moreover, the HCC patients were excluded by the following criteria: (1) patients whose age < 18; (2) patients who combined with other malignancies; (3) patients who lacked critical clinical information; (4) relapsing patients.

Some of HCC patients underwent radical resection or partial resection surgery in Wenzhou Medical University Affiliated Zhoushan Hospital, and their tumor tissues and adjacent normal tissues were also included in the study.

The work involving the serum and tissue specimens was reviewed and approved by the Ethics Committee of Wenzhou Medical University Affiliated Zhoushan Hospital.

Data acquisition from TCGA and GEO

The RNA-Seq expression profiles of 374 HCC patients and 50 normal samples were downloaded from the TCGA database (http://portal.gdc.com), together with corresponding clinicopathological information. The raw read counts of gene expression were normalized in the format of TPM. The clinicopathological information of patients in the TCGA cohort was illustrated in Table S1. Besides, GSE54238 (10 normal livers, 10 chronic inflammatory livers, 10 cirrhotic livers, 26 HCC samples) and GSE121248 (70 HCC tissues and 37 adjacent normal tissues) from the gene expression omnibus (GEO) database (http://www.ncbi.nlm.nih.gov/geo/) were also used for monotonic gene screening.

Principal component analysis (PCA) and differential expression analysis

Principal component analysis (PCA), a data dimensionality reduction method, was carried out with the "prcomp" function and visualized by the "ggplot2" R package. The identification and visualization of the differentially expressed genes (DEGs) in the GEO dataset were conducted by the online tool "GEO2R". The p value was adjusted by Benjamini & Hochberg correction. Log2|FC|> 1 and adjusted $p < 0.05$ were defined as statistically significant for the DEGs. A Venn diagram of the DEGs was constructed using the "VennDiagram" R package, and the intersected DEGs were identified.

Survival analysis

DEGs related with prognosis were screened using univariate Cox analysis (p value < 0.05) and Kaplan–Meier survival analysis (p value < 0.05). Survival data were statistically analyzed using the "survival" R program. Kaplan–Meier curve was visualized using the "survminer" R package, with the median as the cut-off value.

Gene enrichment, protein–protein interaction (PPI) network construction and immune infiltration analysis

The "clusterProfiler" R package (Yu et al. 2012) was applied for Gene Set Enrichment Analysis (GSEA) (Subramanian et al. 2005) to ascertain the different pathways and functions between KPNA2 high and low expression HCC groups. MSigDB (Liberzon et al. 2011) collections were used for predefined gene sets. A PPI network consisting of KPNA2 and its interacting proteins was constructed using the STRING software tool (http://string-db.org) (Szklarczyk et al. 2019).

The most popular strategy for treating unresectable HCC is an immunotherapy based on immune checkpoint inhibitors (ICIs) (He and Xu 2020). So far, there are no reliable biomarkers for predicting the success of immunotherapy for HCC. Hence, immune infiltration of KPNA2 was performed in HCC. The TIMER database (https://cistrome.shinyapps.io/timer/) (Li et al. 2017) was utilized to explore the association between KPNA2 expression and immune cell infiltration and provide the comparison of tumor infiltration levels in HCC with different somatic copy number alterations for KPNA2. Besides, the correlation between KPNA2 expression and three significant immune checkpoint genes (PDCD1, HAVCR2, CTLA4, CD274) was detected by Spearman correlation analysis.

Single-cell RNA-seq (scRNA-seq) analysis

The scRNA-seq dataset (GSE112271) of HCC, which included two patients, was obtained from the GEO database. The R package "Seurat" was utilized to create the object and filter away poor-quality cells. To standardize the library size effect in each cell, scale.factor = 10,000 was used to scale UMI counts. Then the PCA was performed to identify the top 20 principal components (PC) according to the top 2000 highly variable genes. Cluster visualization was performed using UMAP reduction, and the marker genes for each cluster were filtered using the FindAllMarkers function with the adjusted p value < 0.01 and absolute log2 (fold change) value > 1. Finally, the "SingleR" package was utilized to annotate cell types. Besides, Gene expression was represented using "FeaturePlot" and "VlnPlot".

To investigate the biological pathways in which different cell clusters may participate, the average expression values of the cells in different clusters were calculated using the AverageExpression function. The score of the corresponding pathways for each cluster was calculated according to the "GSVA" package (Hanzelmann et al. 2013) and finally visualized by the "pheatmap" package.

Enzyme linked immunosorbent assay (ELISA)

The KPNA2 protein concentration in serum was assessed in duplicate using commercially available ELISA kits (ml060213, MLBio Ltd, China) according to the manufacturer's instructions. The absorbance was read at 450 nm using an enzyme labelling instrument.

Hematoxylin–eosin (HE) staining and immunohistochemistry (IHC)

All specimens were paraffin-embedded, sectioned at a thickness of 4 μm, baked and placed in a fully automated immunohistochemistry instrument (BOND-MAX platform), dewaxed and repaired at 100 °C for 20 min using pH = 9.0 repair solution, peroxidase blocked for 8 min, primary antibody incubated for 25 min at room temperature, horseradish peroxidase-labelled secondary antibody incubated for 8 min at room temperature, DAB color development for 10 min. Hematoxylin re-staining for 8 min, blue return and neutral gum sealing, microscopic observation. The primary antibodies used are as follows: the Ki-67 (1:300, Zhongshan Golden Bridge Biotechnology Ltd, China), p53 (1:600, Zhongshan Golden Bridge Biotechnology Ltd, China), and KPNA2 (1:200, Affinity Bioscience Ltd, China).

Construction of a predictive signature and nomogarm model

The characteristics were selected by univariate and multivariate logistic regression analysis to establish a logistic regression model that can predict the likelihood of developing HCC in CHB or LC patients. A nomogram was created to integrate all predictive characteristics in the logistic regression model using "rms" package, and the area under the curve (AUC) was calculated to measure the model's predictive power. Besides, the calibration curve and decision curve analysis were created to assess the model's stability.

Drug sensitivity analysis

Given that few biomarkers could accurately predict chemotherapeutic drug susceptibility in HCC patients, we predicted the chemotherapeutic response for each sample from the TCGA dataset based on the GDSC database (https://www.cancerrxgene.org/) (Yang et al. 2013) The prediction process was conducted using the R package "pRRophetic". The samples' half-maximal inhibitory concentration (IC50) was estimated by ridge regression.

Docking and molecular dynamics simulations

The protein crystal structures were obtained from the PDB database (https://www.resb.org/pdb), and the 3D structures of four agents were acquired from the PubChem database (https://pubchem.ncbi.nlm.gov). AutoDock Tools (v1.5.7) was used to perform processes such as hydrogenation and charge calculation. The protein center was the docking site to set up the appropriate active pocket and docking parameters. Finally, the receptor protein was docked with the small molecular ligand by performing AutoDock Vina (v1.1.2), and the docking results were visualized by PyMoL (v2.5.4).

Statistical analysis

The patients were stratified into KPNA2-high and KPNA2-low group according to the median cut-off value. Numerical variables that conform to normal distribution and homogeneity of variance were expressed as mean ± standard deviation, and differences between two groups were analyzed using t-test, while numerical variables that do not meet the above conditions were presented as medians (interquartile range [IQR]) and differences between two groups were analyzed using non-parameter analysis. The categorical variables were described as numbers (percentages), and differences between two groups were tested using $\chi 2$ test, while Fisher exact test was used when the expected sample number was less than 5.

All analysis methods and R package were conducted by R (4.0.3) software. A difference of $P < 0.05$ was considered statistically significant (* $p < 0.05$; ** $p < 0.01$; *** $p < 0.001$).

Results

Initial screening for MCDEGs highly correlated with CLH

In GSE54238, PCA revealed no significant difference between normal liver and chronic inflammatory liver, while there was a significant difference between cirrhotic liver and HCC at the transcriptome level (Fig. 1A). We further performed differential expression analysis between chronic inflammatory liver and cirrhotic liver, cirrhotic liver, and HCC, respectively. 3887 DEGs were identified between chronic inflammatory liver and cirrhotic liver (Fig. 1B), including 1834 upregulated genes and 2053 downregulated genes. Between cirrhotic liver and HCC (Fig. 1C), 3485 DEGs were identified, including 1867 upregulated genes and 1618 downregulated genes. After intersecting the above outcomes, we acquired 15 intersected upregulated genes (Fig. 1D) and 15 intersected downregulated genes (Fig. 1E). Besides, the heatmap (Fig. 1F) presented the differential expression of all the intersected genes in GSE54238.

Second screening for MCDEGs highly correlated with CLH

To further demonstrate that these candidate genes obtained from initial screening are related with the course of CLH and may serve as diagnostic or prognostic indicators,

we analyzed the relationship between these common genes and overall survival (OS) in HCC patients. As shown in Fig. 2A–M, we found that 13 candidate genes were correlated with the prognosis of HCC patients by Kaplan–Meier survival analysis, namely, NQO1, FAM72A, TRNP1, HK2, MCM3, KPNA2, ASNS, ZWINT, LOXL4, SLC16A3, HSBP1L1, VIPR1, ADRA1A. Meanwhile, fifteen candidate genes, namely, NQO1, FAM72A, TRNP1, HK2, MCM3, KPNA2, UBE2C, ZWINT, SLC16A3, SULT1C2, MYBL2, HSBP1L1, ISM2, VIPR1, ADRA1A, were associated with the prognosis of HCC patients based on univariate COX regression analysis (Table 1). After combining the above outcomes, we identified 11 common genes linked to the prognosis of HCC patients both in Kaplan–Meier survival and univariate COX regression analysis (Fig. 2N).

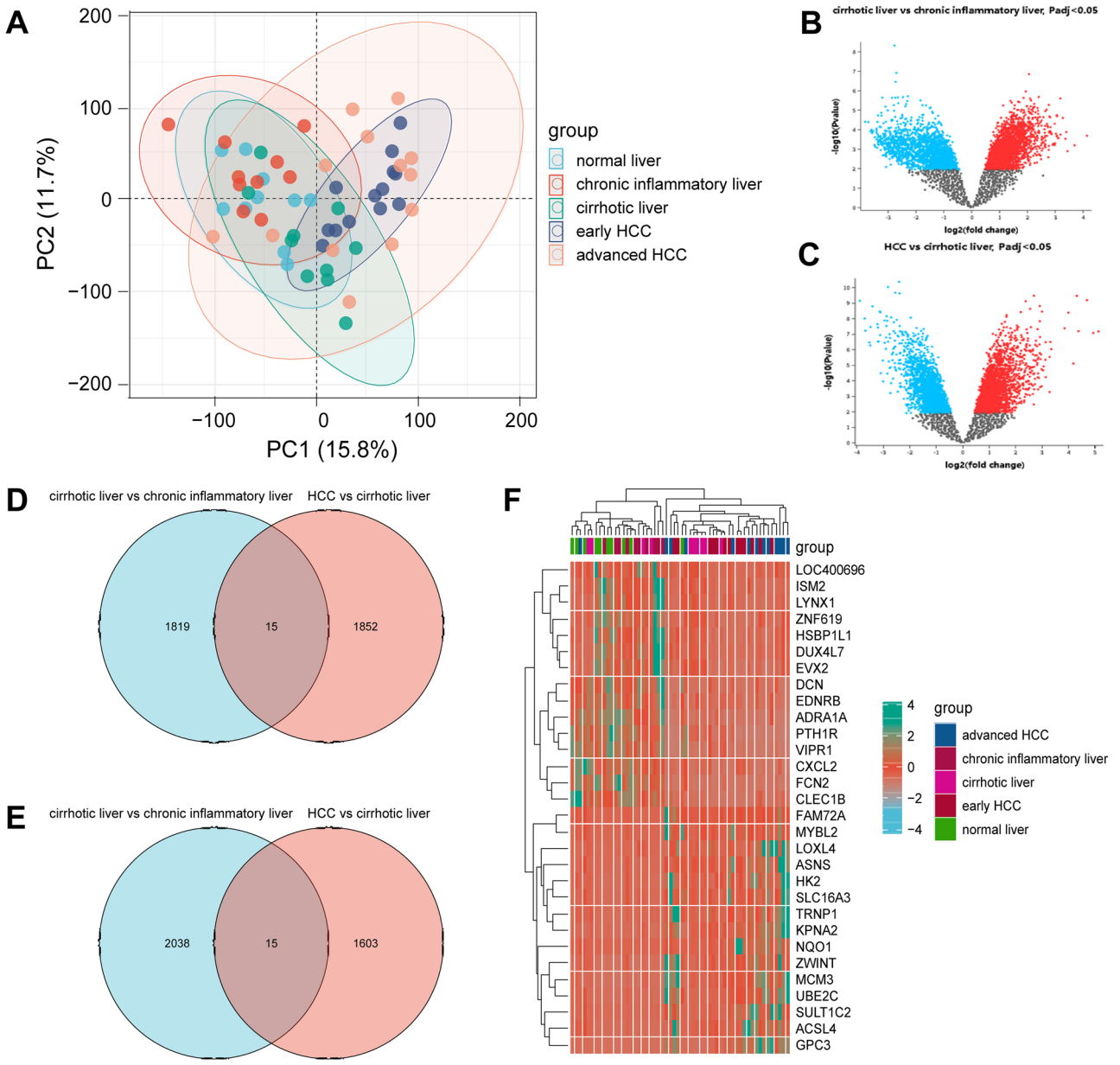

Fig. 1 **A-F** Initial screening for MCDEGs highly correlated with CLH. **A** The PCA plot based on mRNA expression in GSE542348 cohort. **B**, **C** Volcano plot showing DEGs between chronic hepatitis and liver cirrhosis, liver cirrhosis and hepatocellular carcinoma, respectively. **D**, **E** Common upregulated and downregulated DEGs in GSE54238. **F** Heatmap displaying differential expression of the common genes in GSE54238

In addition, the differential expression of all the common genes in the TCGA dataset was presented by the heatmap (Fig. 2O).

Third screening for MCDEGs highly correlated with CLH

To enhance the reliability of the results, we carried out differential expression analysis of the above eleven screened genes in GSE121248. We found that only eight genes screened by the previous two steps, namely, NQO1, FAM72A, MCM3, KPNA2, ZWINT, HSBP1L1, VIPR1, ADRA1A, were still differentially expressed in GSE121248 (Fig. 3A–H). Moreover, the differential expression of eight genes in GSE121248 were presented by the heatmap (Fig. 3I). We also explored the correlation between the expression of eight genes in GSE54238, and the results (Fig. 3J) showed that the expression of eight

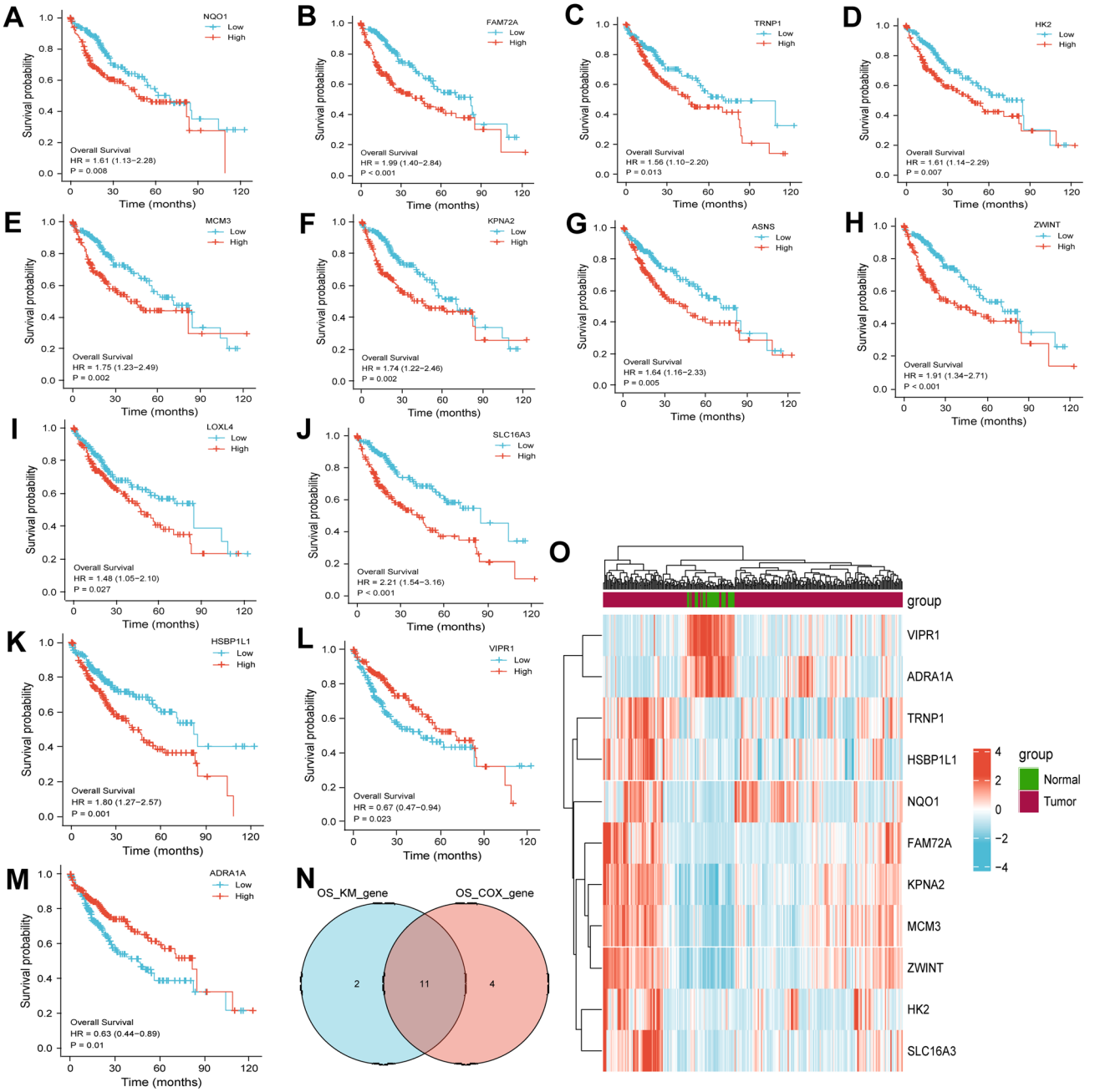

Fig. 2 Second screening for MCDEGs highly correlated with CLH. **A**–**M** The K–M curves of thirteen candidate genes in TCGA dataset. **N** Common candidate genes identified by initial screening were associated with the prognosis of HCC patients in TCGA dataset. **O** Heatmap displaying differential expression of the common genes in TCGA dataset

genes was all closely related with CHB, LC, and HCC, respectively.

Clinical relevance, functional enrichment, PPI network, immune infiltration of KPNA2 in HCC

Since obtaining liver tissue in clinical practice is inconvenient, measuring serum protein levels is more valuable. We found that only the protein expression of NQO1 (mass spectrometry: 490 ng/L), MCM3 (mass spectrometry: 150 ng/L), KPNA2 (mass spectrometry: 160 ng/L) could be detected in the blood based on the HPA database. MCM3 (Mohamed et al. 2022; Li et al. 2020) and NQO1 (Lin et al. 2017) have already been reported to be valuable in the diagnosis and prognosis of HCC and applied in clinical practice. Hence, we mainly focused on KPNA2, and we found that the protein

Table1 Fifteen candidate genes associated with prognosis of HCC patients in TCGA dataset in univariate COX regression analysis

Gene	Hazard ratio (95% CI)	P value
NQO1	1.102 (1.039–1.168)	0.001
FAM72A	2.536 (1.735–3.706)	< 0.001
TRNP1	1.234 (1.129–1.349)	< 0.001
HK2	1.225 (1.095–1.369)	< 0.001
MCM3	1.330 (1.128–1.568)	< 0.001
KPNA2	1.606 (1.360–1.897)	< 0.001
UBE2C	1.281 (1.145–1.433)	< 0.001
ZWINT	1.351 (1.176–1.552)	< 0.001
SLC16A3	1.331 (1.189–1.489)	< 0.001
SULT1C2	1.170 (1.052–1.302)	0.004
MYBL2	1.258 (1.142–1.387)	< 0.001
HSBP1L1	1.390 (1.106–1.747)	0.005
ISM2	1.608 (1.218–2.122)	< 0.001
VIPR1	0.727 (0.558–0.947)	0.018
ADRA1A	0.815 (0.693–0.958)	0.013

expression of KPNA2 was higher in liver cancer tissue than in normal liver tissue according to the HPA database (Fig. 4A). We first investigated the relationship between KPNA2 expression and clinical features performed in HCC. The Sankey diagram (Fig. 4B) showed that high expression of KPNA2 was significantly correlated with TNM stage III, Grade 4, and poor prognosis. We then analyzed differential expression between KPNA2 high and low expression groups and included all DEGs for GSEA. The enriched items that ranked top 6 were "cell cycle" (Fig. 4C), "cell cycle mitotic" (Fig. 4D), "cell cycle checkpoints" (Fig. 4E), "M phase" (Fig. 4F), "metaphase and anaphase" (Fig. 4G), "mitotic prometaphase" (Fig. 4H), indicating that KPNA2 played a crucial role in cell cycle regulation particularly mitosis. Besides, we constructed a PPI network of KPNA2 and the proteins that interact with it (Fig. 4I). To determine the potential of KPNA2 as a biomarker for predicting the efficacy of immunotherapy for HCC, we performed immune infiltration analysis of KPNA2. We discovered that KPNA2 expression was positively correlated with Th2 cell, T helper cell, follicular helper T cell, activated dendritic cell, macrophage, and negatively associated with cytotoxic cell, $CD8^+$ T cell, plasmacytoid dendritic cell, Th17 cell, NK cell (Fig. 4J). More importantly, KPNA2 expression was positively correlated with PDCD1 (Fig. 4K), HAVCR2 (Fig. 4L), CTLA4 (Fig. 4M), while it bore no correlation with CD274 (Fig. 4N). In addition, the SCNA module in TIMER compared tumor infiltration levels in HCC with different somatic copy number alterations for KPNA2. As depicted in the Box plot (Fig. 4O), the infiltration levels of $CD4^+$T cell, macrophage, neutrophil, and dendritic cell varied among each copy number status, including deep deletion, arm-level deletion, diploid/normal, arm-level gain, and high amplification.

Single-cell analysis re-indicated that KPNA2 correlated to immune cell infiltration and participated in cell cycle pathways

Next, we collected one scRNA-seq dataset (GSE112271) to further explore expression profiles of KPNA2 in HCC. As shown in Fig. 5A, the number of genes detected in each cell (nFeature_RNA), the total number of mRNA molecules detected in the cell (nCount_RNA), and the proportion of mitochondrial gene expression in the cell (percent_mt) were performed to remove poor quality cells. The top 2000 highly variable genes were screened for clustering and cell identification (Fig. 5B). Then we applied PCA to reduce the dimensionality based on the similarity of gene expression profiles in cells (Fig. 5C). 13 clusters were identified (Fig. 5D), and 5 immune cell types (dendrite cell, monocyte, neutrophil, B cell, T cell) were annotated (Fig. 5E). Notably, almost only T cells expressed KPNA2 (Fig. 5F), which agreed with the positive correlation between T cell (Th2 cell, T helper cell, follicular helper T cell) and KPNA2 expression. More interestingly, we found that the top4 pathways enriched in T cells were "tumor proliferation signature", "G2M checkpoint", "DNA replication", and "DNA repair" (Fig. 5G), which were all associated with cell cycle and re-proved that KPNA2 may participate in cell cycle modulation.

Diagnostic value of KPNA2 compared with AFP for distinguishing CLH states

The clinical indicator AFP is commonly used to diagnose HCC, so we compared KPNA2 with AFP in distinguishing CLH states (CHB/LC/HCC). As shown in Fig. 6A, serum KPNA2 protein levels monotonically upregulated in CLH (CHB vs LC: $p = 0.0334$;LC vs HCC: $p < 0.0001$). By contrast, there was no significant difference in serum AFP level between CHB patients and LC patients ($p > 0.9999$), while serum AFP level was lower in LC patients than in HCC patients ($p = 0.0047$, Fig. 6B).

To evaluate the diagnostic value of KPNA2 and AFP for classifying different CLH states, we constructed ROC curves and calculated AUC values, sensitivity, specificity, and maximum Youden index for each of these outcomes.

For CHB versus LC, the AUC values of KPNA2 (Fig. 6C) for distinguishing CHB patients from LC patients was 0.838 (95%CI:0.766,0.909), and corresponding sensitivity, specificity, and maximum Youden index were 0.911, 0.721, 0.632 (Table 2). Based on the above data, the recognition efficiency of KPNA2 was surprisingly excellent. By comparison, the AUC value of AFP (Fig. 6D) for separating CHB patients from LC patients was 0.528 (95%CI: 0.423, 0.632),

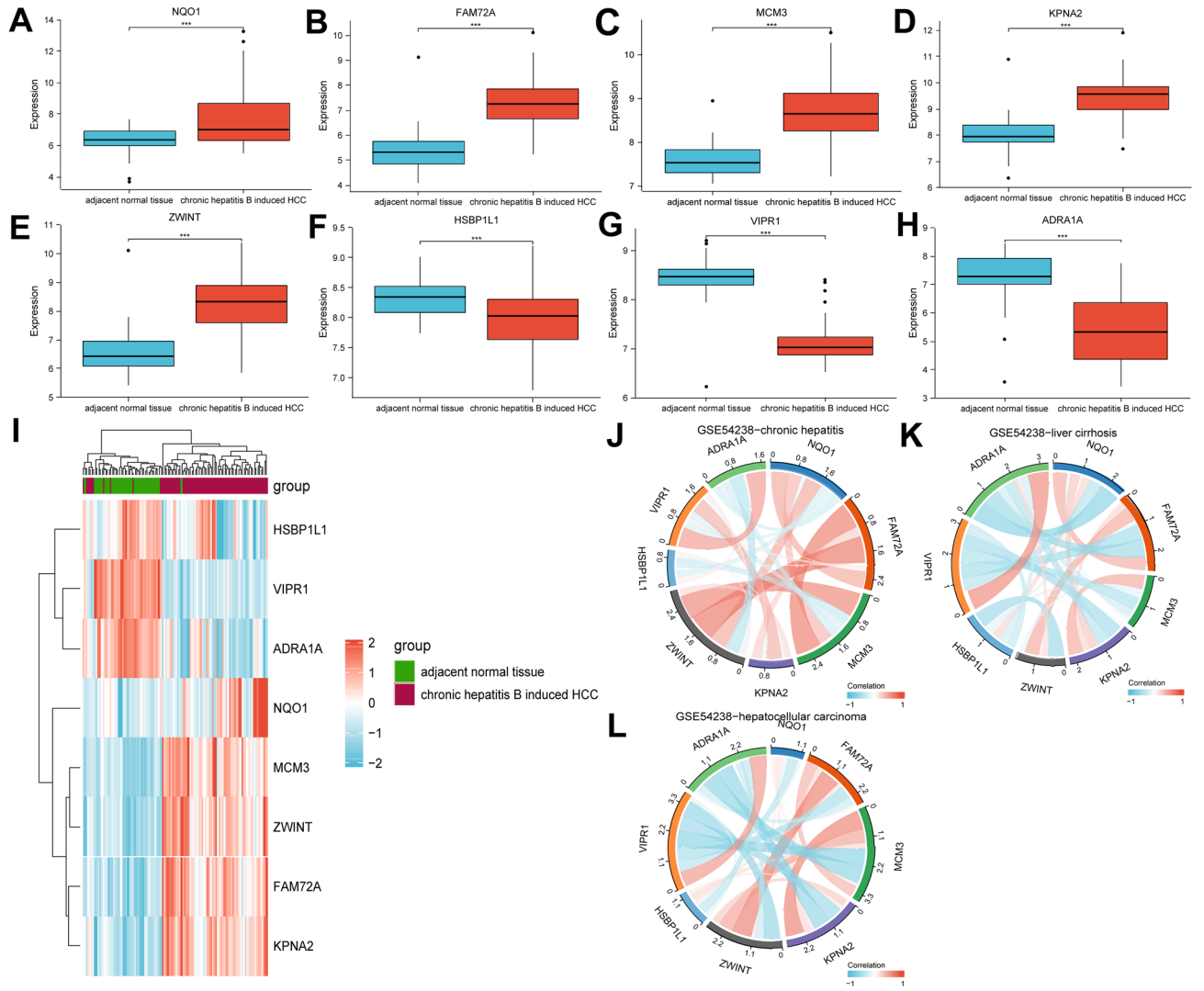

Fig. 3 Third screening for MCDEGs highly correlated with CLH. **A–H** The box plot displaying differential expression of eight genes in GSE121248. **I** Heatmap displaying differential expression of eight genes in GSE54238. **J–L** Chord diagram showing the correlation of eight genes in chronic hepatitis, liver cirrhosis and hepatocellular carcinoma, respectively

suggesting that AFP was almost useless for the identification of CHB patients and LC patients.

For CHB versus HCC, it was worth noting that the AUC values of KPNA2 were higher than that of AFP for telling CHB patients from HCC patients (Fig. 6E,F). Besides, the AUC values (Fig. 6G), sensitivity, and maximum Youden index (Table 2) were markedly improved after combining KPNA2 with AFP using the predicted probability method.

For LC versus HCC, the AUC value of KPNA2 (Fig. 6H) for discriminating LC patients from HCC patients was 0.721 (95%CI:0.622, 0.821), and corresponding sensitivity, specificity and maximum Youden index were 0.667, 0.946, 0.613(Table 2). In contrast, the AUC values of AFP (Fig. 6I) for distinguishing LC patients from HCC patients was 0.830 (95%CI:0.758, 0.902) and its corresponding sensitivity (0.603), specificity (0.929) and maximun youden index(0.532) were all lower than those of KPNA2 (Table 2). Furthermore, the AUC values (Fig. 6J), sensitivity, and maximum Youden index (Table 2) were considerably improved after combining KPNA2 with AFP, which was very meaningful because the early detection of HCC patients had more effective treatment options.

Associations between serum KPNA2 expression and prognostic variables in CHB patients

When compared with prognostic variables in CHB patients (Table S2), high KPNA2 expression was significantly correlated with HBeAg(+) (39.3%, p = 0.0326), higher ALT level (24.00[17.00, 35.00] U/L, p = 0.0187), higher liver stiffness

level (7.85[6.20, 8.73] Kpa, p = 0.0007), all of which suggested the poor prognosis for CHB patients and the potential for CHB evolving into LC. In addition, high KPNA2 expression tended to be more frequently linked to higher BMI level (23.18 ± 2.57 kg/m^2, p = 0.3899), lower platelet level (144.80 ± 17.52 × 10^9/L, p = 0.4019), higher glucose level (5.43[5.09, 5.79] mmol/L, p = 0.2072) and higher fat attenuation level (238.60 ± 40.92 dB/m, p = 0.3212) though these associations didn't reach statistical significance.

Associations between serum KPNA2 expression and prognostic variables in LC patients

When compared with prognostic variables in LC patients (Table S3), high KPNA2 expression was significantly related to lower hemoglobin level (79.54 ± 27.20 g/L, p < 0.0001), lower platelet level (97.39 ± 69.14 × 10^9/L, p = 0.0316), lower albumin level (29.61 ± 6.11 g/L, p < 0.0001), higher glucose level (7.00[5.24,8.90] mmol/L, p = 0.0345), higher Child–Pugh score (p < 0.0001), higher gastrointestinal bleeding incidence (71.43%, p = 0.0005) and higher hepatic encephalopathy incidence (28.57%, p = 0.0218), all of which indicated poor prognosis and serious condition of CL patients. Besides, high KPNA2 expression showed a tendency to be more frequently linked to higher creatinine level (73.70[57.13,112.38] g/L, p = 0.0631), higher infection incidence(17.86%, p = 0.1927), and higher portal vein thrombosis incidence(14.29%, p = 0.3516) though these associations did not reach statistical significance.

Associations between serum KPNA2 expression and prognostic variables in HCC

When compared with prognostic variables in HCC patients (Table S4), high KPNA2 expression was significantly associated with lower albumin level (36.76 ± 5.97 g/L, p = 0.0178), lower high-density lipoprotein level (0.86 ± 0.32 mmol/L, p = 0.0345), higher cancer thrombus incidence (25.00%, p = 0.0265), more advanced stage(34.48%, p = 0.0184), higher grade (57.89%, p = 0.0163), higher microvascular invasion incidence (47.37%, p = 0.0033), higher Ki-67 positive rate (28.57%, p = 0.0450), and higher Child–Pugh score (p = 0.0347). In addition, the protein levels of KPNA2 in HCC tissues were detected by IHC. Differential expression of KPNA2 in HCC tissues of different histologic grades, microvascular invasion, and Ki-67 positive rate were shown in Fig. 7.

Construction of a predictive signature and nomogarm model for CLH

To predict the likelihood of developing HCC in CHB patients or LC patients, we established a binary logistic regression model (one group was CHB patients and LC patients, and the other was HCC patients). Based on univariate and multivariate logistic regression analysis, four independent risk factors, namely, KPNA2 expression (OR = 1.001, p < 0.001), gender (OR = 0.017, p = 0.001), age (OR = 1.191, p < 0.001), and AFP (OR = 1.077, p = 0.006), were included in the model (Table3). We incorporated these factors into nomogram establishment (Fig. 8A) and conducted ROC analysis to evaluate the predictive capacity of the model. Of note, we converted KPNA2 expression, age, AFP into dichotomous variables to enhance the aesthetic and application value of the nomogram. Results from AUC value (0.959, 95%CI:0.934–0.984; Fig. 8B), calibration (Fig. 8C), and decision curve analysis (Fig. 8D) suggested a tremendous predictive capacity and clinical validity of the nomogram model.

Drug sensitivity analysis for HCC patients with different KPNA2 expression

To explore the possible application of KPNA2 in chemotherapy or targeted therapy of HCC patients, we estimated the IC_{50} of four commonly used chemotherapeutic or targeted drugs by combining drug sensitivity and gene expression profiling data. The spearman's correlation analysis suggested that KPNA2 expression was negatively correlated with IC_{50} values of 5-fluorouracil ($p = 3.48 \times e^{-25}$, $\rho_{spearman} = -0.50$;Fig. 9A), doxorubicin ($p = 1.64 \times e^{-7}$, $\rho_{spearman} = -0.27$; Fig. 9B), gemcitabine ($p = 8.16 \times e^{-28}$, $\rho_{spearman} = -0.53$; Fig. 9C), sorafenib ($p = 4.79 \times e^{-13}$, $\rho_{spearman} = -0.36$; Fig. 9D).

Considering the good correlation between KPNA2 expression and drug sensitivity of four agents, we further implemented molecular docking analysis to evaluate the binding energy and binding favorability. The results revealed that the binding free energy of KPNA2-5-fluorouracil complex (Fig. 9E), KPNA2-doxorubicin complex (Fig. 9F), KPNA2-gemcitabine complex (Fig. 9G), KPNA2-sorafenib complex (Fig. 9H) were – 5.0 kcal/mol, – 7.6 kcal/mol, – 6.1 kcal/mol, – 7.2kacl/mol, respectively. Taken together, the four agents all exhibited excellent binding affinity to KPNA2.

Discussion

As one of the most prevalent cancers in the world, HCC has a complex biological development that involves several genes, multiple factors, and multiple stages of progression. CLH, also known as "liver cancer trilogy", is the most crucial step in the evolution of HCC in China. Despite the increasing number of early screening and diagnostic markers for liver cancer being uncovered (Dalbeni et al. 2023;

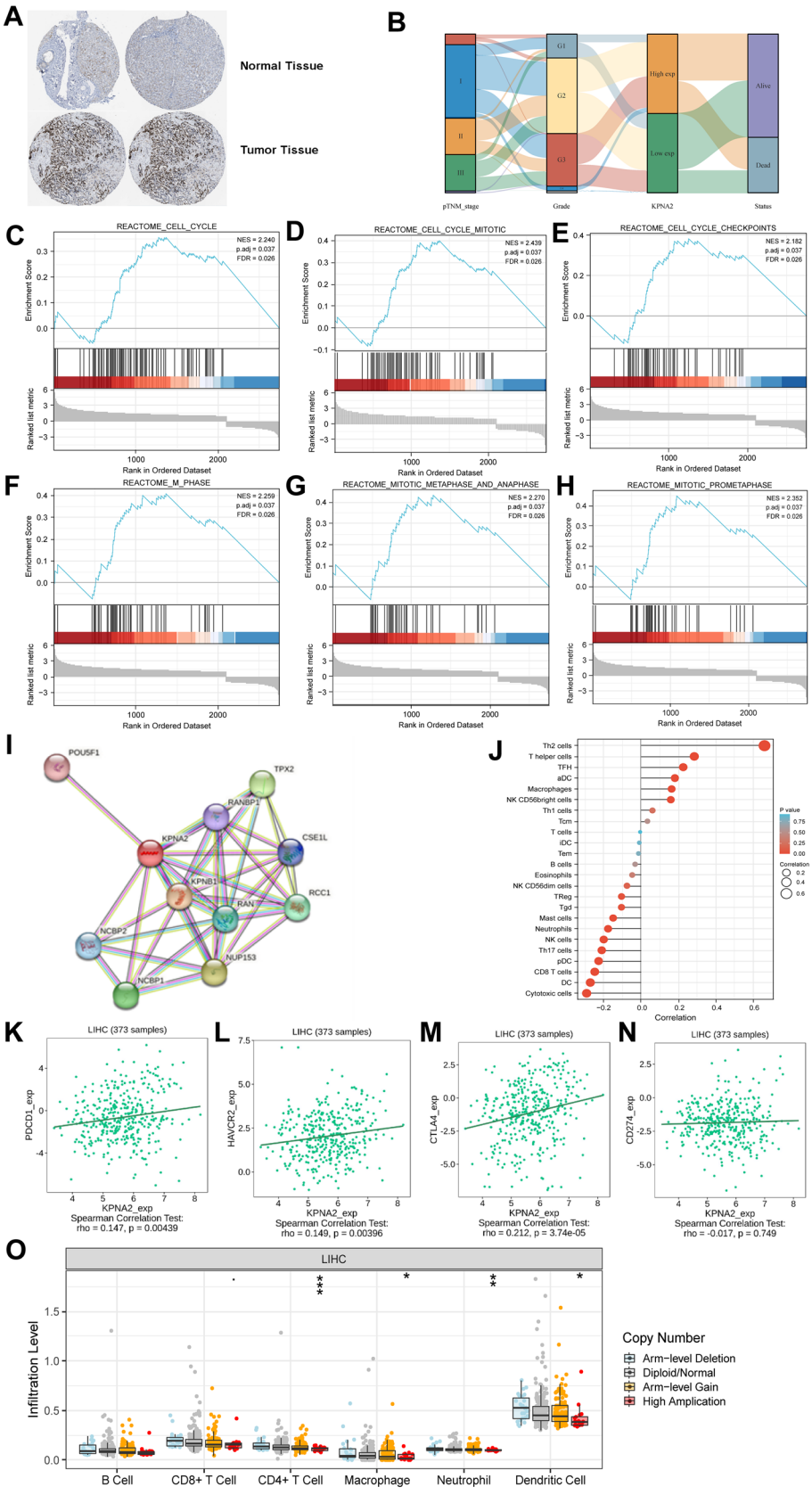
A
Normal Tissue
Tumor Tissue
B
pTNM_stage
Grade
KPNA2
Status
C
REACTOME_CELL_CYCLE
D
REACTOME_CELL_CYCLE_MITOTIC
E
REACTOME_CELL_CYCLE_CHECKPOINTS
F
REACTOME_M_PHASE
G
REACTOME_MITOTIC_METAPHASE_AND_ANAPHASE
H
REACTOME_MITOTIC_PROMETAPHASE
Enrichment Score
Ranked list metric
Rank in Ordered Dataset
I
POU5F1
TPX2
RANBP1
KPNA2
CSE1L
KPNB1
RAN
RCC1
NCBP2
NUP153
NCBP1
J
Correlation
P value
K
L
M
N
LIHC (373 samples)
PDCD1_exp
HAVCR2_exp
CTLA4_exp
CD274_exp
KPNA2_exp
O
LIHC
Infiltration Level
B Cell
CD8+ T Cell
CD4+ T Cell
Macrophage
Neutrophil
Dendritic Cell
Copy Number
Arm−level Deletion
Diploid/Normal
Arm−level Gain
High Amplication

◂**Fig. 4** Bioinformatic analysis of KPNA2 in HCC. **A** Differential expression between normal liver tissue and liver cancer tissue based on HPA database(immunohistochemistry). **B** The Sankey diagram showing relationship between KPNA2 expression and clinical features. **C–H** The GSEA of DEGs between KPNA2 high and low expression groups. **I** PPI network of KPNA2 generated by STRING. **J** Association between KPNA2 expression and immune cell infiltration levels in LIHC. **K–N** Association between KPNA2 expression and immune checkpoint genes (PDCD1, HAVCR2, CTLA4, CD274) in LIHC. **O** The box plot presenting the distributions of each immune subset at each copy number status in LIHC. LIHC, Liver Hepatocellular Carcinoma

Miao et al. 2023; Cai et al. 2023) previous studies have only focused on the end stage of HCC and neglected the progression of CLH as a disease process. Therefore, the diagnostic sensitivity and specificity of these biomarkers were not yet optimal and were not useful for early prediction of the disease course and prevention of HCC. Our work identified a significant MCDEG, namely KPNA2, using comprehensive analysis of scRNA-seq and bulk RNA-seq and verified its differential expression in serum level. Moreover, we found that serum KPNA2 expression was correlated with some poor prognostic factors in CHB, LC, and HCC, respectively. In addition, we thoroughly explored its diagnostic value for distinguishing different CLH states and established a nomogram model for predicting CLH progression. Finally, we revealed the association between KPNA2 expression and IC50 of chemotherapeutic drugs for HCC.

We first performed differential expression analysis in GSE54238 and identified 30 intersected DEGs. After Kaplan–Meier survival and univariate COX regression analysis, we screened 11 intersected DEGs. We further analyzed differential expression in GSE121248 and finally identified 8 MCDEGs highly correlated with CLH. Since liver tissue is not easily accessible in clinical practice, measuring serum protein levels is more practical. Among 8 MCDEGs, only NQO1, MCM3, and KPNA2 could be detected in the blood based on the HPA database. As MCM3 and NQO1 have already been reported to be valuable in the diagnosis and prognosis of HCC, we chose KPNA2 for subsequent research. The GSEA showed that the top 6 enriched pathways were "cell cycle", "cell cycle mitotic", "cell cycle checkpoints", "M phase", "metaphase and anaphase", "mitotic prometaphase", indicating that KPNA2 was involved in cell cycle process in HCC. The immune infiltration analysis revealed that KPNA2 expression was positively correlated with Th2 cell, T helper cell, follicular helper T cell and negatively linked to cytotoxic cell, $CD8^+$ T cell, plasmacytoid dendritic cell. We also found that KPNA2 expression was significantly associated with three significant immune checkpoints-PDCD1, HAVCR2 and CTLA4. The tumor immune microenvironment, including many immune cells and immunomodulators, can influence the efficacy of immune checkpoint inhibitors (ICIs) (Mehraj et al. 2021; Zhu et al. 2023). The absence of immune cell infiltration in tumor microenvironment is one of the principal constraints of current ICIs therapies. Many studies have focused on identification of biomarkers that could predict immunotherapeutic response effectively for clinical purpose (Ghahremanloo et al. 2019). For example, an 18-miRNA-based signature was constructed to give a valuable reference for ICIs treatment in colon adenocarcinoma. (Xue et al. 2021) and a immune-associated gene model was established to predict the efficacy of ICIs treatment in stomach adenocarcinoma (Xue et al.2022). Considering that KPNA2 expression was highly associated with immune cell infiltration and the expression of three critical immune checkpoint genes, KPNA2 could be a potential biomarker for ICIs therapy in HCC.

On the other hand, scRNA-seq analysis revealed that KPNA2 was mainly expressed in T cells, and the top4 pathways enriched in T cells were "tumor proliferation signature", "G2M checkpoint", "DNA replication", and "DNA repair", which re-indicated that KPNA2 was correlated with immune cell infiltration and participated in cell cycle pathway. Prior research has also demonstrated that KPNA2 strongly affected genes linked to the cell cycle and DNA replication in HCC (Yu et al. 2021). This engagement may be related to its participation as a nucleoplasmic protein transporter in various cellular biological processes. For example, Gao et al. discovered that KPNA2 expression accelerated the cell cycle in HCC via increasing CCNB2 and CDK1 (Gao et al. 2018).

To further investigate the diagnostic and prognostic value of KPNA2 in CHB, LC, and HCC, respectively, we first tested KPNA2 expression levels in our serum samples using ELISA and found that serum KPNA2 protein levels monotonically upregulated in CLH. Based on AUC values, sensitivity, specificity, and maximum Youden index, KPNA2 performed better than AFP in distinguishing CHB patients from LC patients, LC patients from HCC patients. It was noteworthy that AFP was almost useless for identification of CHB patients and LC patients. AFP had a better AUC value than KPNA2 in distinguishing LC patients from HCC patients, while KPNA2 performed better concerning sensitivity. Indeed, sensitivity was more important for diagnosing HCC patients because HCC was a disease with a poor prognosis, severe consequences of missed diagnosis, and early surgical resection can lead to better treatment results. Hence, KPNA2 had a more excellent application value than AFP for diagnosing HCC. Besides, sensitivity was considerably improved after combining KPNA2 with AFP, which may bridge the gap between single indicators in the diagnosis of HCC.

Later, we explored the associations between serum KPNA2 expression and prognostic variables in CHB, LC, and HCC, respectively. We discovered that high serum

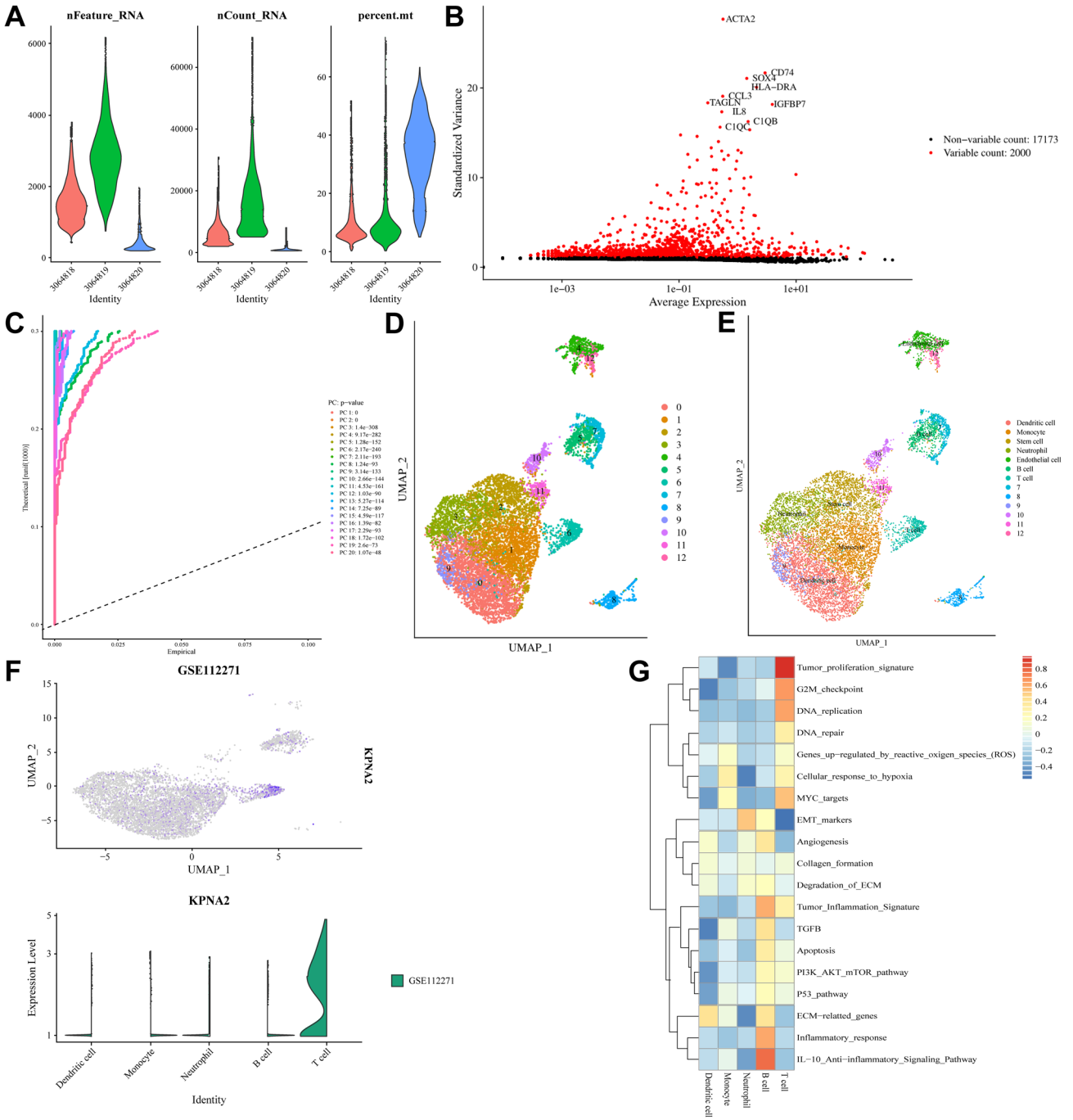

Fig. 5 Analysis of single cell sequence data from multiregional sample in HCC. **A** Quality control assessment and data filtering of single cell sequence data. **B** Highly variable genes used for clustering and cell identification. **C** Top 20 principal components were identified based on P value < 0.05. **D** Different cell clusters visualized by UMAP reduction. **E** Corresponding annotation of the cell clusters. **F** KPNA2 expression between different immune cell clusters. **G** The pathways highly enriched in different immune cell clusters

KPNA2 expression was significantly correlated with many poor prognostic indicators in CHB, LC, and HCC, respectively. Thus, using serum KPNA2 expression, a better prognosis indication and risk stratification of patients can be achieved. For HCC, interestingly, high KPNA2 expression was significantly associated with a higher Ki-67 positive rate and microvascular invasion. Ki-67 is a tumor proliferation-associated antigen, and high expression of Ki-67 means rapid tumor growth and severe disease (Huang et al. 2022). Microvascular invasion refers to the nesting mass of cancer

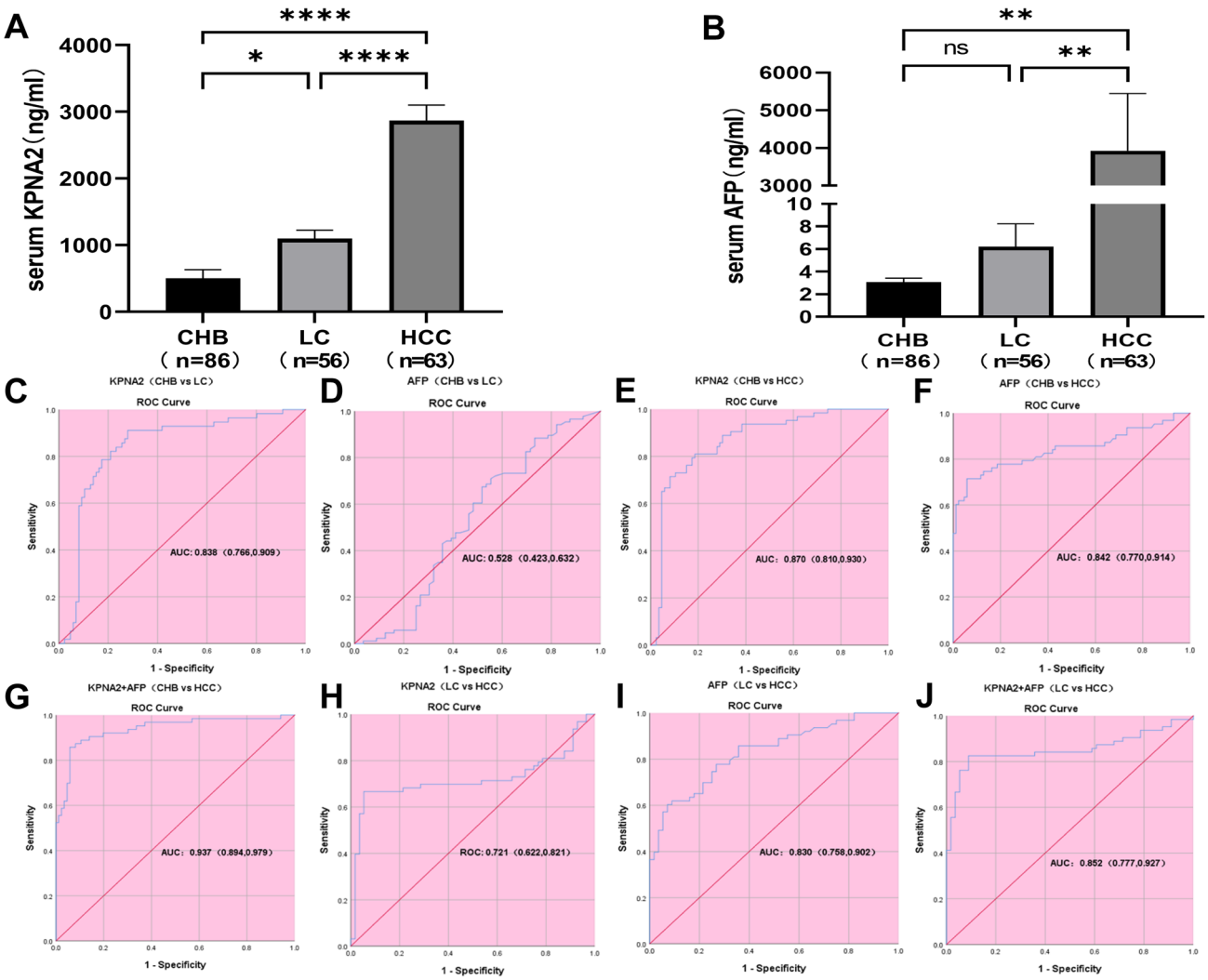

Fig. 6 Diagnostic value of KPNA2 compared with AFP for distinguishing CLH states. Expression level of serum KPNA2 (**A**) and serum AFP (**B**) in different CLH states. For CHB vs LC, ROC curve analysis of KPNA2 (**C**) and AFP (**D**). For CHB vs HCC, ROC curve analysis of KPNA2 (**E**), AFP (**F**) and KPNA2 + AFP (**G**). For LC vs HCC, ROC curve analysis of KPNA2 (**H**), AFP (**I**) and KPNA2 + AFP (**J**). (* $p < 0.05$; ** $p < 0.01$; *** $p < 0.001$)

Table2 Evaluation indicators of classifiers for distinguishing CLH states

Name	Classifier	AUC	Sensitivity	Specificity	Maximum Youden index
CHB vs LC	KPNA2	0.838	0.911	0.721	0.632
	AFP	0.528	0.482	0.674	0.157
CHB vs HCC	KPNA2	0.870	0.714	0.919	0.633
	doAFP	0.842	0.714	0.942	0.656
	(KPNA2 + AFP)[a]	0.937	0.857	0.942	0.799
LC vs HCC	KPNA2	0.721	0.667	0.946	0.613
	AFP	0.830	0.603	0.929	0.532
	(KPNA2 + AFP)[b]	0.852	0.825	0.911	0.736

[a]Algorithm, logit (P) = 0.001*KPNA2 + 0.147*AFP-2.699

[b]Algorithm, logit (P) = 0.001*KPNA2 + 0.03*AFP-2.099

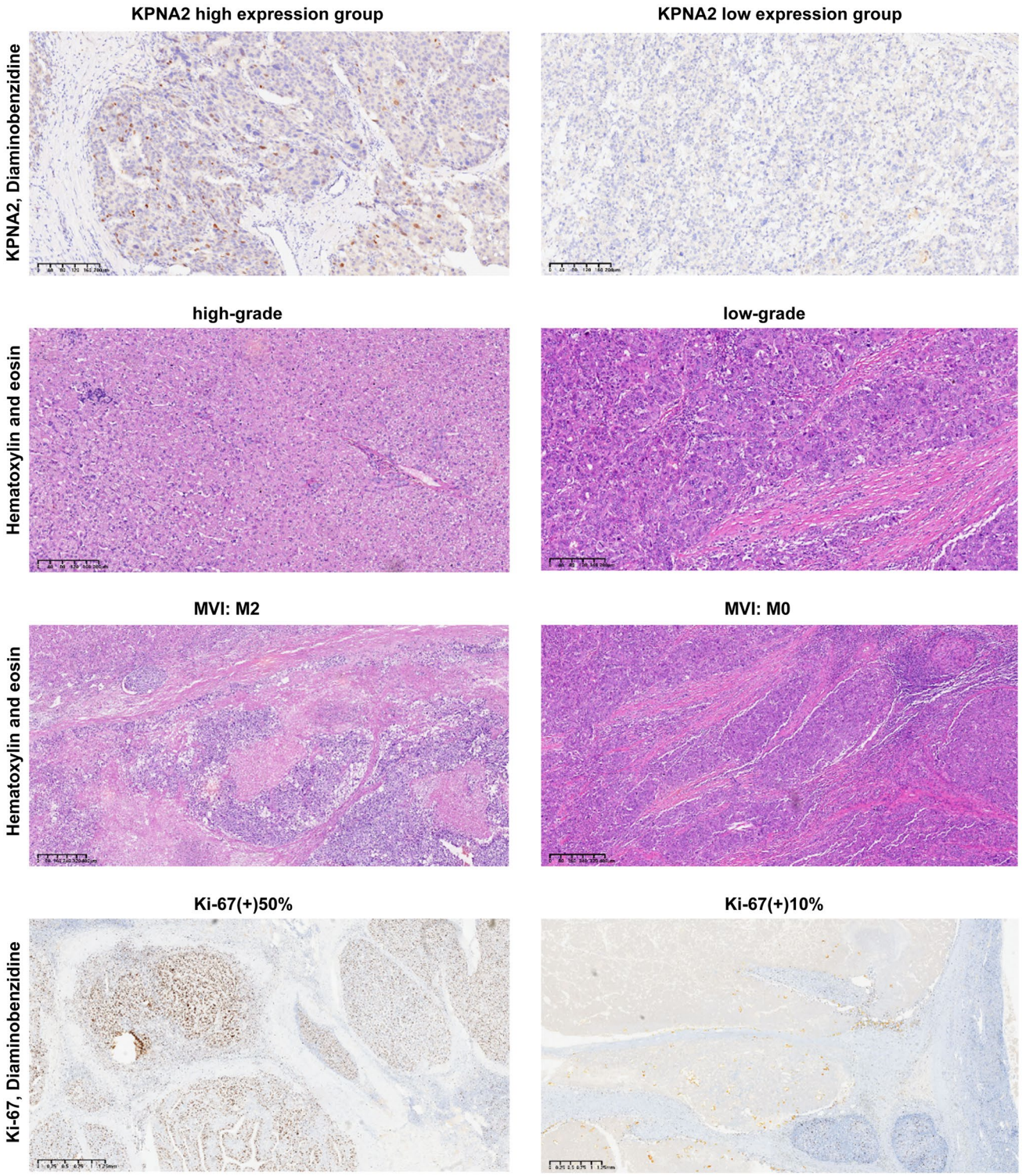

Fig. 7 Differential expression of KPNA2 in HCC tissues of different histologic grades, microvascular invasion, and Ki-67 positive rate. Left column(KPNA2 high expression group):KPNA2 high expression/high-grade/MVI:M2/Ki-67(+)50%; Right column(KPNA2 low expression group): KPNA2 low expression/low-grade/MVI:M0/Ki-67(+)10%. MVI: microvascular invasion

Table 3 Binary logistic regression analysis to identify statistically significant characteristics

Characteristics	Univariate logistic analysis		Multivariate logistic analysis	
	OR (95% CI)	P value	OR (95% CI)	P value
KPNA2 expression	1.001 (1.001, 1.001)	**< 0.001**	1.001 (1.001, 1.001)	**< 0.001**
Gender	5.268 (2.235, 12.419)	**< 0.001**	0.017 (0.002, 0.176)	**0.001**
Hypertension	0.328 (0.159, 0.678)	**0.003**	2.086 (0.423, 10.301)	0.367
Diabetes	0.439 (0.210, 0.919)	**0.029**	2.571 (0.636, 10.393)	0.185
Age	1.082 (1.044, 1.122)	**< 0.001**	1.191 (1.088, 1.303)	**< 0.001**
BMI	1.125 (1.023, 1.236)	**0.015**	1.130 (0.902, 1.415)	0.289
AFP	1.057 (1.023, 1.092)	**0.001**	1.077 (1.022, 1.136)	**0.006**
WBC	1.028 (0.911, 1.159)	0.658		
Hb	1.001 (0.991, 1.010)	0.905		
PLT	0.997 (0.993, 1.002)	0.198		
AST	1.017 (1.005, 1.029)	**0.006**	1.004 (0.994, 1.014)	0.481
ALT	1.010 (1.000, 1.019)	**0.046**	1.003 (0.998, 1.019)	0.702
TBil	1.006 (0.999, 1.014)	0.116		
Creatinine	1.004 (0.994, 1.014)	0.414		
Albumin	0.944 (0.908, 0.981)	**0.003**	1.048 (0.960, 1.144)	0.299

BMI body mass index; *AFP* alpha-fetoprotein;*WBC* white blood cell; *Hb* hemoglobin; *PLT* platelet; *AST* aspartate aminotransferase; *ALT* alanine aminotransferase; *TBil* total bilirubin

cells seen microscopically in the lumen of endothelium-lined vessels, which can be used as a prognostic indicator of tumors (Ballard 2023). These findings agreed with the outcomes of earlier experiments. Drucker et al. demonstrated that KPNA2 could increase stathmin expression, which contributes to the metastasis and invasion of HCC cells (Drucker et al. 2019). Jiang et al. also discovered that overexpression of nuclear KPNA2 indicated the early recurrence and poor prognosis in patients with HCC after hepatectomy (Jiang et al. 2014).

To predict the likelihood of developing HCC in CHB patients or LC patients, we established a binary logistic regression model consisting of 4 independent risk factors (KPNA2 expression, gender, age, AFP). Then we incorporated these factors into nomogram establishment, and the AUC value of ROC curve was 0.959, which exhibited extremely excellent predictive capacity. In addition, we found that KPNA2 expression was negatively correlated with IC_{50} values of 5-fluorouracil, doxorubicin, gemcitabine, and sorafenib, suggesting that HCC patients with high KPNA2 expression may benefit from these chemotherapeutic drugs. This data supported the idea that KPNA2 would likely be a key target for the treatment of HCC in the future.

KPNA2, in recent years, has been recognized as a biomarker for malignancies. Previous research has demonstrated that it contributed to the promotion of malignant features in various cancer types (Wang et al. 2011; Sakai et al. 2010; Han and Wang 2020). Nevertheless, rare reports on the involvement of KPNA2 in HCC can be found. KPNA2 plays an essential role in nucleoplasmic transport (Christiansen and Dyrskjøt 2013). The investigators suggested that the nuclear KPNA2 expression might provide a selective advantage in the emergence of HCC. Zhong et al. showed that KPNA2 encourages the proliferation and invasion of HCC by in vitro tests employing several cell lines (Lin et al. 2018). Unfortunately, little was known about the molecular mechanism behind KPNA2's involvement in the onset and progression of HCC. Thus, our study highlighted the role of KPNA2 in several aspects of CLH, which helped to elaborate on the involvement of KPNA2 in HCC progression.

There are still some areas for improvement in the study. First, this study was only a retrospective study, and further prospective studies with a sufficiently large sample scale are required to corroborate each other. Second, additional in vivo and in vitro experiments are essential to clarify the molecular mechanism underlying KPNA2's effects on the progression of CLH.

In conclusion, we, for the first time, developed a holistic approach to research the CLH process from the perspective of MCDEGs. KPNA2 was a significant MCDEG highly correlated with CLH and was valuable for distinguishing different CLH states. We demonstrated that serum KPNA2 expression was correlated with many poor prognostic

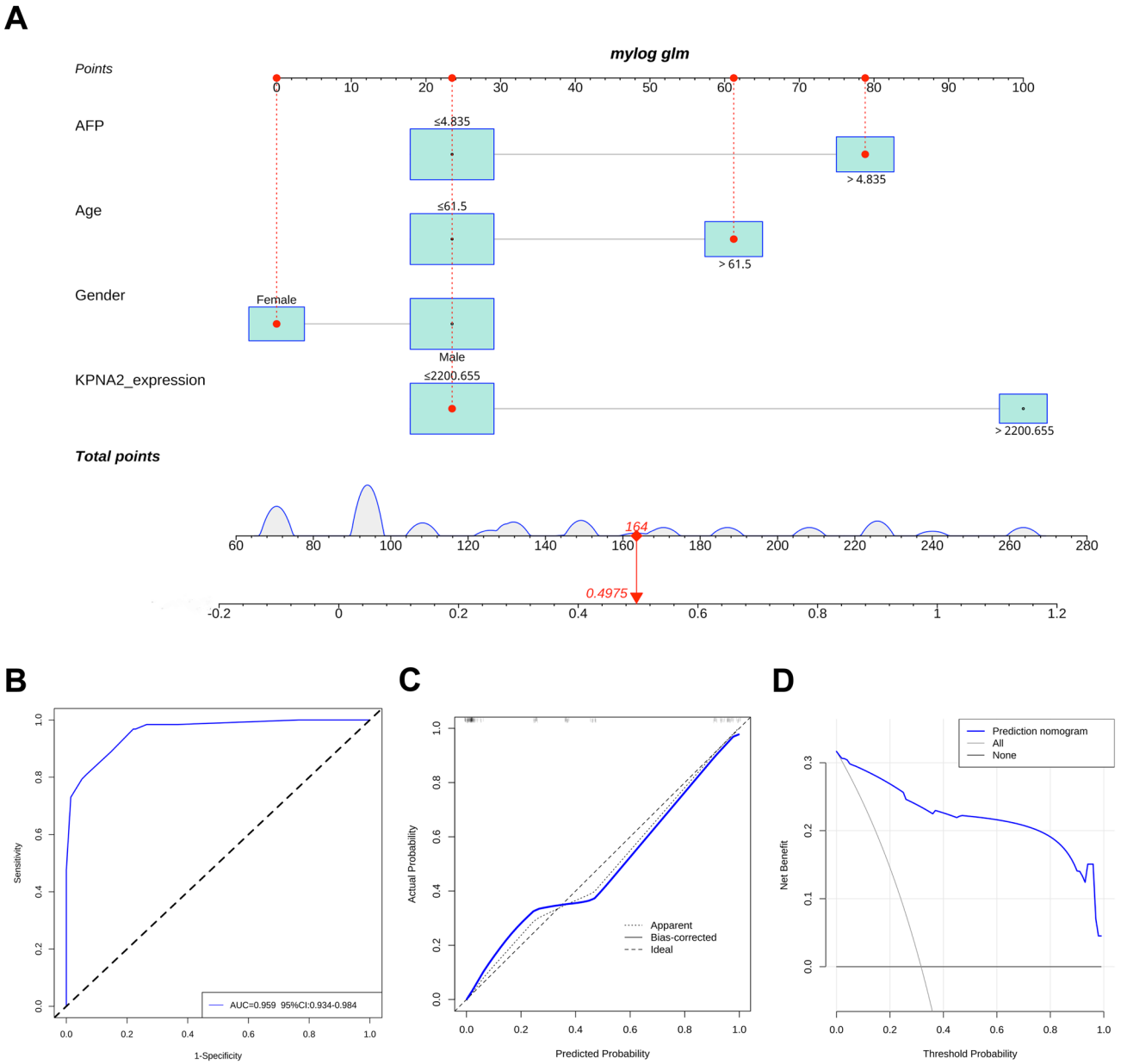

Fig. 8 A predictive model was established for CLH. **A** The nomogram combining four independent risk factors was developed for predicting the occurrence of HCC. The predicive ability of nomogram were tested by ROC analysis (**B**), Calibration curve (**C**) and Decision curve analysis (**D**)

variables in CHB, LC, and HCC, respectively. In addition, a predictive nomogram consisting of four independent indicators was constructed for CLH. We also found that KPNA2 expression was negatively correlated with IC_{50} values of four chemotherapeutic drugs in HCC, namely, 5-fluorouracil, doxorubicin, gemcitabine, and sorafenib. Therefore, this work provided a new serum biomarker for diagnosing different CLH states, monitoring the dynamic evolution of CLH, and a new therapeutic target for intervening in the progression of CLH.

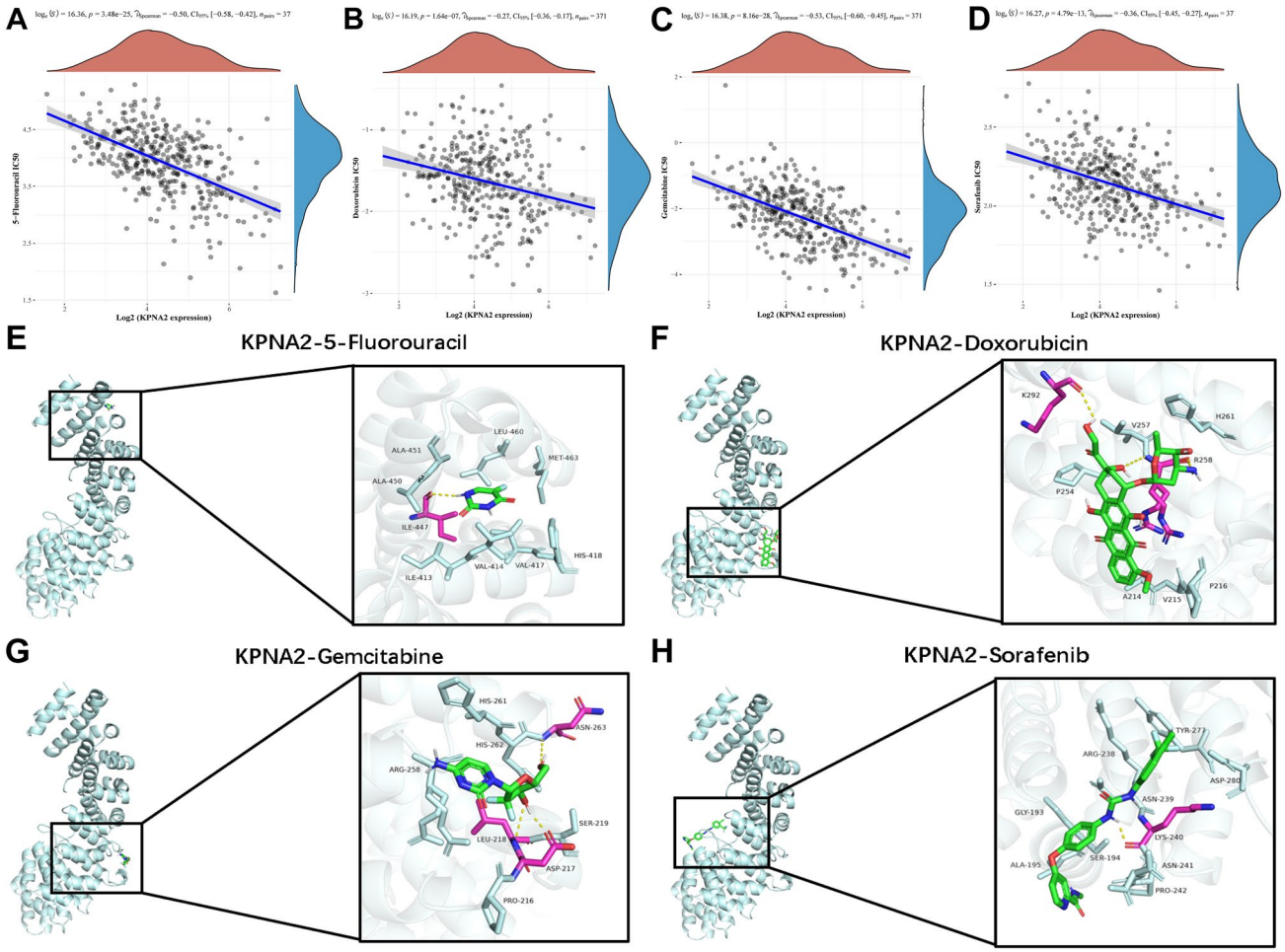

Fig. 9 Drug sensitivity analysis for HCC patients with different KPNA2 expression. Association between KPNA2 expression and IC_{50} values of 5-fluorouracil (**A**), doxorubicin (**B**), gemcitabine (**C**), sorafenib (**D**), respectively. Molecular docking simulation outcomes of KPNA2-5-fluorouracil complex (**E**), KPNA2-doxorubicin complex (**F**), KPNA2-gemcitabine complex (**G**), KPNA2-sorafenib complex (**H**)

Supplementary Information The online version contains supplementary material available at https://doi.org/10.1007/s00432-023-05213-z.

Author contributions YP and YZ initiated the study and organized it; YP and ZL designed and carried out bioinformatics analyses, statistical analyses, drew figures, and drafted the manuscript; DJ completed immunohistochemistry experiments, SL contributed to the review and editing. All authors have read and agreed to the published version of the manuscript.

Funding This work was supported by Zhejiang Province Major Science and Technology Project for Medicine and Health, grant number WKJ-ZJ-2329; General Scientific Research Project of Zhejiang Provincial Education Department, grant number Y202250086.

Data availability The original contributions presented in the study are included in the article/Supplementary Material. Further inquiries can be directed to the corresponding author. Publicly available datasets were analyzed in this study. This data can be found here: https://portal.gdc.cancer.gov/, and http://www.ncbi.nlm.nih.gov/geo/.

Declarations

Conflict of interest The authors declare that they have no conflict of interest.

Ethical approval The work involving the serum and tissue specimens was reviewed and approved by the Ethics Committee of Wenzhou Medical University Affiliated Zhoushan Hospital. Informed consent was obtained from each patient included in the present study.

References

Ballard DH (2023) Microvascular invasion in hepatocellular carcinoma: bridging the global gap between imaging and clinical practice. Acad Radiol. https://doi.org/10.1016/j.acra.2023.05.017

Cai X, Tang D, Chen J et al (2023) Evaluation of serum FGL1 as diagnostic markers for hbv-related hepatocellular carcinoma. Lab Med 54:270–281. https://doi.org/10.1093/labmed/lmac094

Cassany A, Guillemain G, Klein C et al (2004) A karyopherin alpha2 nuclear transport pathway is regulated by glucose in hepatic and pancreatic cells. Traffic 5:10–19. https://doi.org/10.1046/j.1398-9219.2003.0143.x

Chen T, Liu R, Niu Y et al (2021) HIF-1α-activated long non-coding RNA KDM4A-AS1 promotes hepatocellular carcinoma progression via the miR-411–5p/KPNA2/AKT pathway. Cell Death Dis 12:1152. https://doi.org/10.1038/s41419-021-04449-2

Christiansen A, Dyrskjøt L (2013) The functional role of the novel biomarker karyopherin α 2 (KPNA2) in cancer. Cancer Lett 331:18–23. https://doi.org/10.1016/j.canlet.2012.12.013

Dalbeni A, Natola LA, Garbin M et al (2023) Interleukin-6: a new marker of advanced-sarcopenic HCC cirrhotic patients. Cancers (basel) 15:2406. https://doi.org/10.3390/cancers15092406

Drucker E, Holzer K, Pusch S et al (2019) Karyopherin α2-dependent import of E2F1 and TFDP1 maintains protumorigenic stathmin expression in liver cancer. Cell Commun Signal 17:159. https://doi.org/10.1186/s12964-019-0456-x

Gao CL, Wang GW, Yang GQ et al (2018) Karyopherin subunit-α 2 expression accelerates cell cycle progression by upregulating CCNB2 and CDK1 in hepatocellular carcinoma. Oncol Lett 15:2815–2820. https://doi.org/10.3892/ol.2017.7691

Ghahremanloo A, Soltani A, Modaresi SMS et al (2019) Recent advances in the clinical development of immune checkpoint blockade therapy. Cell Oncol (dordr) 42:609–626. https://doi.org/10.1007/s13402-019-00456-w

Guo X, Wang Z, Zhang J et al (2019) Upregulated KPNA2 promotes hepatocellular carcinoma progression and indicates prognostic significance across human cancer types. Acta Biochim Biophys Sin (shanghai) 51:285–292. https://doi.org/10.1093/abbs/gmz003

Han Y, Wang X (2020) The emerging roles of KPNA2 in cancer. Life Sci 241:117140. https://doi.org/10.1016/j.lfs.2019.117140

Hanzelmann S, Castelo R, Guinney J (2013) GSVA: gene set variation analysis for microarray and RNA-seq data. BMC Bioinformatics 14:7. https://doi.org/10.1186/1471-2105-14-7

He X, Xu C (2020) Immune checkpoint signaling and cancer immunotherapy. Cell Res 30:660–669. https://doi.org/10.1038/s41422-020-0343-4

Hsu YC, Huang DQ, Nguyen MH (2023) Global burden of hepatitis B virus: current status, missed opportunities and a call for action. Nat Rev Gastroenterol Hepatol. https://doi.org/10.1038/s41575-023-00760-9

Huang Z, Zhou P, Li S et al (2022) Prediction of the Ki-67 marker index in hepatocellular carcinoma based on dynamic contrast-enhanced ultrasonography with sonazoid. Insights Imaging 13:199. https://doi.org/10.1186/s13244-022-01320-6

Jiang P, Tang Y, He L et al (2014) Aberrant expression of nuclear KPNA2 is correlated with early recurrence and poor prognosis in patients with small hepatocellular carcinoma after hepatectomy. Med Oncol 31:131. https://doi.org/10.1007/s12032-014-0131-4

Li X, Sun Y, Jin Y (2008) Identification of karyopherin-alpha 2 as an Oct4 associated protein. J Genet Genom 35:723–728. https://doi.org/10.1016/S1673-8527(08)60227-1

Li T, Fan J, Wang B et al (2017) TIMER: a web server for comprehensive analysis of tumor-infiltrating immune cells. Cancer Res 77:e108–e110. https://doi.org/10.1158/0008-5472

Li HT, Wei B, Li ZQ et al (2020) Diagnostic and prognostic value of MCM3 and its interacting proteins in hepatocellular carcinoma. Oncol Lett 20:308. https://doi.org/10.3892/ol.2020.12171

Liberzon A, Subramanian A, Pinchback R et al (2011) Molecular signatures database (MSigDB) 3.0. Bioinformatics 27(12):1739–1740. https://doi.org/10.1093/bioinformatics/btr260

Lim DH, Casadei-Gardini A, Lee MA et al (2022) Prognostic implication of serum AFP in patients with hepatocellular carcinoma treated with regorafenib. Future Oncol 18:3021–3030. https://doi.org/10.2217/fon-2022-0524

Lin L, Sun J, Tan Y et al (2017) Prognostic implication of NQO1 overexpression in hepatocellular carcinoma. Hum Pathol 69:31–37. https://doi.org/10.1016/j.humpath.2017.09.002

Lin CZ, Ou RW, Hu YH (2018) Lentiviral-mediated microRNA-26b up-regulation inhibits proliferation and migration of hepatocellular carcinoma cells. Kaohsiung J Med Sci 34:547–555. https://doi.org/10.1016/j.kjms.2018.05.00

Malaguarnera G, Giordano M, Paladina I et al (2010) Serum markers of hepatocellular carcinoma. Dig Dis Sci 55:2744–2755. https://doi.org/10.1007/s10620-010-1184-7

Mehraj U, Ganai RA, Macha MA et al (2021) The tumor microenvironment as driver of stemness and therapeutic resistance in breast cancer: new challenges and therapeutic opportunities. Cell Oncol (dordr) 44:1209–1229. https://doi.org/10.1007/s13402-021-00634-9

Mehta N (2020) Hepatocellular carcinoma-how to determine therapeutic options. Hepatol Commun 4:342–354. https://doi.org/10.1002/hep4.1481

Miao LL, Wang JW, Liu HH et al (2023) Hypomethylation of glycine dehydrogenase promoter in peripheral blood mononuclear cells is a new diagnostic marker of hepatitis B virus-associated hepatocellular carcinoma. Hepatobiliary Pancreat Dis Int 23:S1499-3872(23)00034–6. https://doi.org/10.1016/j.hbpd.2023.02.011

Mohamed AS, Abd El Hafez A, Eltantawy A et al (2022) Diagnostic and prognostic value of isolated and combined MCM3 and glypican-3 expression in hepatocellular carcinoma: a novel immunosubtyping prognostic model. Appl Immunohistochem Mol Morphol 30:694–702. https://doi.org/10.1097/PAI.0000000000001080

O'Brien P, Morin P Jr, Ouellette RJ et al (2011) The Pax-5 gene: a pluripotent regulator of B-cell differentiation and cancer disease. Cancer Res 71:7345–7350. https://doi.org/10.1158/0008-5472

Pinter M, Trauner M, Peck-Radosavljevic M et al (2016) Cancer and liver cirrhosis: implications on prognosis and management. ESMO Open 1:e000042. https://doi.org/10.1136/esmoopen-2016-000042

Qu Q, Sawa H, Suzuki T et al (2004) Nuclear entry mechanism of the human polyomavirus JC virus-like particle: role of importins and the nuclear pore complex. J Biol Chem 279:27735–27742. https://doi.org/10.1074/jbc.M310827200

Sakai M, Sohda M, Miyazaki T et al (2010) Significance of karyopherin-{alpha} 2 (KPNA2) expression in esophageal squamous cell carcinoma. Anticancer Res 30:851–856

Stroffolini T, Stroffolini G (2023) A historical overview on the role of hepatitis B and C viruses as aetiological factors for hepatocellular carcinoma. Cancers (basel) 15:2388. https://doi.org/10.3390/cancers15082388

Subramanian A, Tamayo P, Mootha VK et al (2005) Gene set enrichment analysis: a knowledge-based approach for interpreting genome-wide expression profiles. Proc Natl Acad Sci USA 102(43):15545–15550. https://doi.org/10.1073/pnas.0506580102

Sung H, Ferlay J, Siegel R et al (2021) global cancer statistics 2020: GLOBOCAN estimates of incidence and mortality worldwide for 36 cancers in 185 countries. CA A Cancer J Clin 71:209–249. https://doi.org/10.3322/caac.21660

Szklarczyk D, Gable AL, Lyon D et al (2019) STRING v11: protein-protein association networks with increased coverage, supporting functional discovery in genome-wide experimental datasets. Nucleic Acids Res 47:D607–D613. https://doi.org/10.1093/nar/gky1131

Tanaka T, Taniguchi T, Sannomiya K et al (2013) Novel des-γ-carboxy prothrombin in serum for the diagnosis of hepatocellular carcinoma. J Gastroenterol Hepatol 28:1348–1355. https://doi.org/10.1111/jgh.12166

Wang CI, Wang CL, Wang CW et al (2011) Importin subunit alpha-2 is identified as a potential biomarker for non-small cell lung cancer by integration of the cancer cell secretome and tissue

transcriptome. Int J Cancer 128:2364–2372. https://doi.org/10.1002/ijc.25568
Wang JH, Zhong XP, Zhang YF et al (2017) Cezanne predicts progression and adjuvant tace response in hepatocellular carcinoma. Cell Death Dis 8:e3043–e. https://doi.org/10.1038/cddis.2017.428
Wang P, Zhao Y, Liu K et al (2019) Wip1 cooperates with KPNA2 to modulate the cell proliferation and migration of colorectal cancer via a p53-dependent manner. J Cell Biochem 120:15709–15718. https://doi.org/10.1002/jcb.28840
Xu M, Xu K, Yin S et al (2023) In-depth serum proteomics reveals the trajectory of hallmarks of cancer in hepatitis B virus-related liver diseases. Mol Cell Proteomics 22:100574. https://doi.org/10.1016/j.mcpro.2023.100574
Xue W, Wang Y, Xie Y et al (2021) miRNA-based signature associated with tumor mutational burden in colon adenocarcinoma. Front Oncol 11:634841. https://doi.org/10.3389/fonc.2021.634841
Xue W, Dong B, Wang Y et al (2022) A novel prognostic index of stomach adenocarcinoma based on immunogenomic landscape analysis and immunotherapy options. Exp Mol Pathol 128:104832. https://doi.org/10.1016/j.yexmp.2022.104832
Yang W, Soares J, Greninger P et al (2013) Genomics of drug sensitivity in cancer (GDSC): a resource for therapeutic biomarker discovery in cancer cells. Nucleic Acids Res 41:D955–D961. https://doi.org/10.1093/nar/gks1111
Yu C, Wang L, Han Y et al (2012) clusterProfiler: an R package for comparing biological themes among gene clusters. Omics A J Integr Biol 16:284–287. https://doi.org/10.1089/omi.2011.0118
Yu B, Liang H, Ye Q et al (2021) Establishment of a genomic-clinicopathologic nomogram for predicting early recurrence of hepatocellular carcinoma after R0 resection. J Gastrointest Surg 25:112–124. https://doi.org/10.1007/s11605-020-04554-1
Zan Y, Wang B, Liang L et al (2019) MicroRNA-139 inhibits hepatocellular carcinoma cell growth through down-regulating karyopherin alpha 2. J Exp Clin Cancer Res 38:182. https://doi.org/10.1186/s13046-019-1175-2
Zhang Y, Zhang M, Yu F et al (2015) Karyopherin alpha 2 is a novel prognostic marker and a potential therapeutic target for colon cancer. J Exp Clin Cancer Res 34:145. https://doi.org/10.1186/s13046-015-0261-3
Zhang J, Zhang X, Wang L et al (2021) Multiomics-based analyses of KPNA2 highlight its multiple potentials in hepatocellular carcinoma. Peer J 9:e12197. https://doi.org/10.7717/peerj.12197
Zhu YH, Zheng JH, Jia QY et al (2023) Immunosuppression, immune escape, and immunotherapy in pancreatic cancer: focused on the tumor microenvironment. Cell Oncol (dordr) 46:17–48. https://doi.org/10.1007/s13402-022-00741-1